Effects of an Axial Amino Ligand on the Spectroscopic and Electrochemical Properties of Amino(methoxo)-(tetraphenylporphyrinato)antimony(V) Complexes

Shin-ichiro Tsunami,[1] Kousuke Tanaka,[2] Jin Matsumoto,[2] Tsutomu Shiragami,*[2] and Masahide Yasuda[2]

[1]Miyazaki Prefecture Environmental Science Association, 6258-20 Tayoshi, Miyazaki 880-0911

[2]Department of Applied Chemistry, Faculty of Engineering, University of Miyazaki, Gakuen-Kibanadai, Miyazaki 889-2192

Received October 1, 2007; E-mail: t0g109u@cc.miyazaki-u.ac.jp

We investigated the effects of an axial amino ligand on the spectroscopic and electrochemical properties of alkylamino(methoxo)(tetraphenylporphyrinato)antimony(V) bromide **1** and anilino(methoxo)(tetraphenylporphyrinato)antimony(V) bromide **2**. Fluorescence measurements of **1** and **2** showed that their fluorescence quantum yields were lower than that of dihydroxo(tetraphenylporphyrinato)antimony(V) bromide (**3**) due to intramolecular electron transfer (ET) from the axial amino ligand to the excited porphyrin ring. Fluorescence was enhanced by the addition of a proton, which was caused by the protonation of the axial nitrogen atom, thereby preventing ET. From the titration curves of fluorescence quantum yield (Φ_f) versus proton concentration, we estimated the acid dissociation constants (pK_a) for the conjugate acid of the axial amino ligand of **1** to be 4.41–5.03. The reduction potentials ($E_{1/2}^{red}$) of **2** depended strongly on the electronic effect of the *p*-substituents (X) on the axial aniline group whereas the $E_{1/2}^{red}$ of methoxo(*p*-substituted-phenoxo)(tetraphenylporphyrinato)antimony(V) bromide was little affected by the *p*-substituents on the phenoxo ligand. These observations were interpreted as reflecting the participation of the axial amino ligand in the LUMO, calculated for **2** by the PM3 method.

Recently, the synthesis and characterization of metalloporphyrin complexes have been extensively investigated from the viewpoint of light-energy conversion processes involving photocatalysis[1–3] and dye-sensitized solar cell systems.[4,5] Among a number of metalloporphyrin complexes synthesized so far, it is well known that high-valent metalloporphyrin complexes of Ge^{IV}, Sn^{IV}, P^{V}, As^{V}, and Sb^{V} can covalently connect to axial ligands through carbon, oxygen, nitrogen, and sulfur atoms,[6] which differs from the behavior of transition-metal porphyrin complexes.[7–10] We have paid especially close attention to tetraphenylporphyrinatoantimony(V) complexes (Sb(tpp)) with functionalized moieties on their axial ligands. We have already reported their photocatalytic properties[11–13] and photoinduced intramolecular electron and energy transfer between the porphyrin ring and the axial ligands.[13] Most studies on Sb(tpp) have been performed using Sb(tpp) coordinated with an oxygen atom as an axial ligand.[14–21] However, there have been no systematic studies on the electrochemistry or photochemistry of Sb(tpp) coordinated with axial amino ligands, although the synthesis and structural characterization of these complexes have been reported previously.[6,22]

Here we report the effect of axial amino ligands on the spectroscopic and electrochemical properties of alkylamino-(methoxo)(tetraphenylporphyrinato)antimony(V) bromide **1** and anilino(methoxo)(tetraphenylporphyrinato)antimony(V) bromide **2** (Scheme 1).

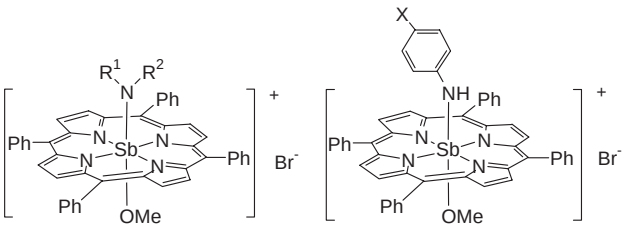

	R^1	R^2
1a	H	$C_6H_5CH_2$-
1b	H	$HO(CH_2)_3$-
1c	H	$CH_3(CH_2)_3$-
1d	H	*iso*-Pr-
1e	H	*tert*-Bu-
1f	-$(CH_2)_4$-	

	X
2a	NC
2b	CF_3
2c	Cl
2d	H
2e	Me
2f	MeO

Scheme 1. Amino(methoxo)(tetraphenylporphyrinato)antimony(V) complexes **1** and **2**.

Results

Synthesis of Sb(tpp) Complexes with an Amino Group as an Axial Ligand. Introduction of axial ligands into high-valent metalloporphyrin has usually been performed by exchanging axial halogen ligands with nucleophiles.[14,23–26] As a reference sample, dihydroxo(tetraphenylporphyrinato)antimony(V) bromide (**3**) was prepared by the hydrolysis of dibromo(tetra-

Published on the web May 14, 2008; doi:10.1246/bcsj.81.583

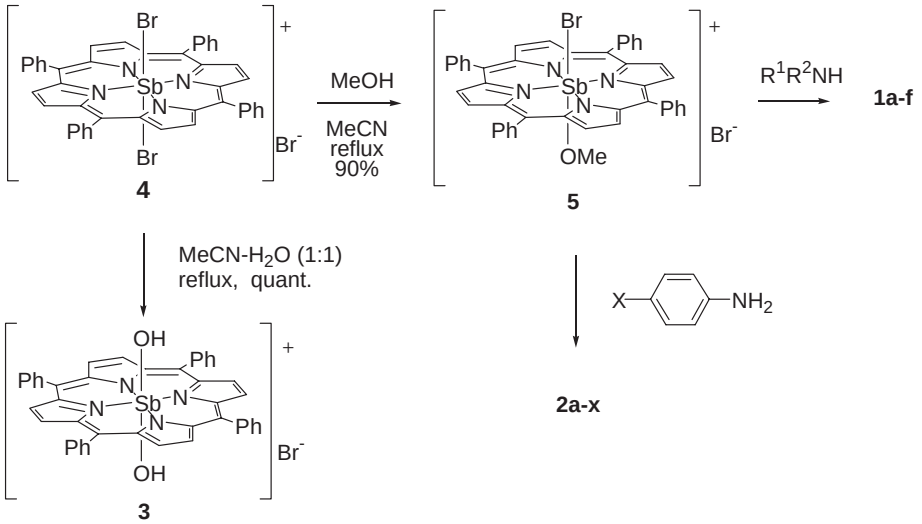

Scheme 2. Synthetic route of **1**–**3**.

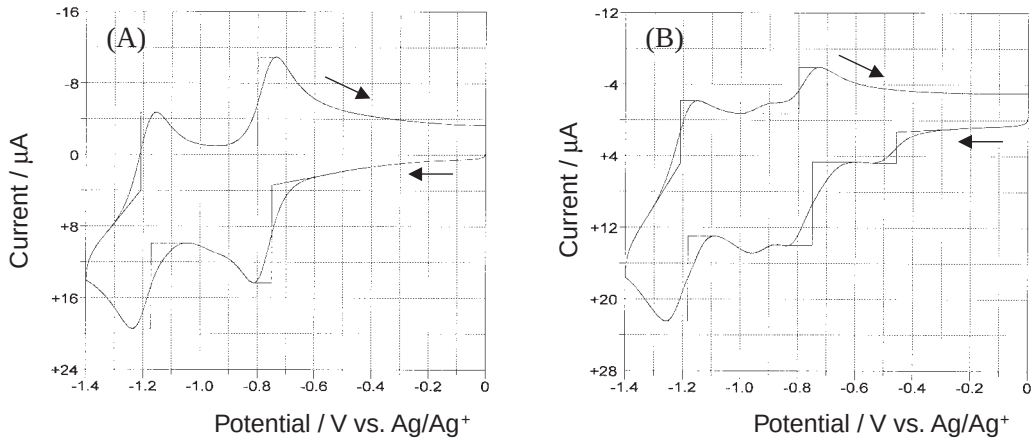

Figure 1. Cyclic voltammogram of **1d** in (A) MeCN and in (B) MeCN in the presence of $HClO_4$ (5.5×10^{-5} mol dm^{-3}).

phenylporphyrinato)antimony(V) bromide (**4**). The reaction of **4** with amines, however, gave free base tetraphenylporphyrin (H_2(tpp)) because the amines performed well as electron donors to reduce **4** to the Sb^{III} complex, which underwent demetallation easily.[20] As starting materials, therefore, we used bromo(methoxo)(tetraphenylporphyrinato)antimony(V) bromide (**5**), which has more negative reduction potential than **4**; $E_{1/2}{}^{red}$ vs. SCE = −0.36 V for **5** and −0.23 V for **4**.

The reaction of **5** with aliphatic amines successfully produced the corresponding alkylamino(methoxo)(tetraphenylporphyrinato)antimony(V) **1a**–**1e** in relatively good yield (>70%), although **1f** was only obtained in poor yield due to decomposition during purification on silica gel (Scheme 2). Similarly, **5** reacted with *p*-substituted anilines to produce *p*-substituted anilino(methoxo)(tetraphenylporphyrinato)antimony(V) **2a**–**2e**. However, the reaction of **5** with tertiary amines such as Et_3N and Bu_3N produced H_2(tpp), because of the strong reducing abilities of these amines. In the case of bifunctional amine 3-amino-1-propanol, coordination occurred selectively at the amino group, while no reaction occurred at the hydroxy group. This was confirmed by X-ray crystallographic analysis of **1b** in addition to assignment by NMR spectra (Scheme 3).

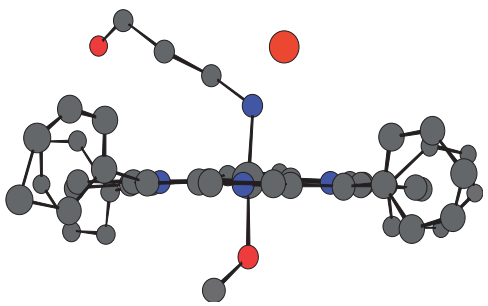

Scheme 3. Crystal structure of **1b**.

Electrochemical Properties. A typical example is the cyclic voltammogram (CV) of **1d** in MeCN, where reversible first and second reduction peaks were observed at −0.52 and −0.94 V, respectively, as shown in Figure 1A. The same CV profiles were also observed in other complexes **1** and **2**. The first and second reduction peaks of **1** and **2** were reversible, because the ratio (i_{pc}/i_{pa}) of the peak current intensity during a cathodic sweep (i_{pc}) to that during an anodic sweep (i_{pa}) was measured to be 0.8–1.0, and the peak potential differences between the cathodic and anodic sweeps, which were predicted

Table 1. Spectroscopic and Electrochemical Data of Sb(tpp) Complexes **1**–**3** in MeCN

	$E_{1/2}^{ox}$/V[a]	$E_{1/2}^{red}$/V[b]	pK_a[c]	Absorption spectra	Fluorescence spectra		ΔG/eV[g]	Yield/%[h]
				λ_{max}/nm (log ε)[d]	λ_{max}/nm[e]	$\Phi_f \times 10^2$ [f]		
1a	1.33	−0.50, −0.90	4.30	422 (5.40), 556 (4.11), 596 (3.96)	594, 645	0.96		73
1b	1.40	−0.51, −0.90	5.02	419 (5.54), 553 (4.20), 594 (4.01)	594, 645	1.00		70
1c	1.41	−0.51, −0.91	5.03	421 (5.52), 556 (4.17), 596 (4.03)	594, 645	1.00		73
1d	1.33	−0.52, −0.94	4.41	421 (5.51), 556 (4.19), 596 (4.05)	594, 645	0.37		76
1e	1.33	−0.49, −0.94	4.84	419 (5.36), 553 (4.05), 593 (3.85)	594, 645	1.00		73
1f	1.42	−0.53, −0.95	5.02	419 (5.57), 553 (4.13), 594 (3.98)	596, 646	0.18		31
2a	1.23 (1.03)[i]	−0.48, −0.88	—	420 (5.40), 556 (4.08), 597 (3.92)	594, 645	2.09	−0.37	18
2b	1.23 (1.00)[i]	−0.42, −0.82	—	421 (5.27), 557 (3.85), 599 (3.70)	594, 645	2.26	−0.43	18
2c	1.12 (0.72)[i]	−0.54, −0.94	—	419 (5.61), 551 (4.22), 590 (3.95)	594, 645	0.38	−0.42	19
2d	1.03 (0.68)[i]	−0.55, −0.95	—	420 (5.44), 557 (4.11), 598 (3.98)	594, 654	1.24	−0.50	86
2e	0.78 (0.52)[i]	−0.56, −0.96	—	421 (5.27), 557 (3.85), 599 (3.70)	594, 645	0.84	−0.74	20
2f	0.76 (0.34)[i]	−0.57, −0.97	—	421 (5.51), 557 (4.00), 599 (3.82)	594, 645	0.83	−0.75	20
3	1.40	−0.51, −0.91	—	417 (5.62), 550 (4.49), 590 (4.30)	596, 646	5.18		100

a) Half peak of oxidation potentials vs. SCE. b) Half peak of reduction potentials vs. SCE. c) Acid dissociation constants for conjugated acid of axial amino ligand. d) The absorption maximum of Sb(tpp) chromophore. e) The emission maxima in the fluorescence spectra of Sb(tpp) chromophore under excitation at 420 nm. f) The fluorescence quantum yields of Sb(tpp) chromophore in MeCN under excitation of Soret band at 420 nm. g) The free energy change for the electron transfer from axial ligands to Sb(tpp) at S_1 state: $E^{0-0} = 2.08$ eV. h) Product yield from **5**. i) The $E_{1/2}^{ox}$ of axial anilino ligands. The values in parenthesis are the $E_{1/2}^{ox}$ of the corresponding substituted aniline.

theoretically, were between 40 and 80 mV. Furthermore, the differences (ΔE) between the first reduction peaks and the second reduction peaks were 0.43–0.48 V. The half peaks of the reduction potentials ($E_{1/2}{}^{red}$) and the oxidation potentials ($E_{1/2}{}^{ox}$) of **1** and **2** are summarized in Table 1. The $E_{1/2}{}^{red}$ of **1** was close to that of **3**, independent of the axial ligands. The $E_{1/2}{}^{red}$ of **2** varied from −0.42 (X = CF_3) to −0.57 V (X = OMe), depending on the substituents (X) of the anilino ligands. The reversible reduction process of **1** and **2** can be attributed to the successive valence change from Sb^V to Sb^{III}.[21] On the other hand, the $E_{1/2}{}^{ox}$ of **1** and **2** did not show a reversible peak. Although the $E_{1/2}{}^{ox}$ of **1a**–**1f** were almost the same as that of **3**, the $E_{1/2}{}^{ox}$ of **2a**–**2f** varied from 1.23 (X = CF_3) to 0.76 V (X = OMe), depending on X, and lied between that of the corresponding substituted anilines and that of **3**. This suggests that axial anilino ligands interacted with the porphyrin ring in HOMO levels in **2**.

Absorption and Fluorescence Properties. Absorption and fluorescence spectral data of **1**, **2**, and **3** are summarized in Table 1. Although the absorption maxima (λ_{max}) of **1** and **2** were observed at slightly longer wavelengths than that of **3**, the axial coordination of nitrogen atoms to antimony atoms caused no significant spectral changes for the Soret band or the Q-band. The absorption spectra of **2** were essentially similar to those of **3**, except for the appearance of an extra band due to the axial anilino ligand at wavelengths shorter than 300 nm.

Photoexcitation of **1** and **2** gave weak fluorescence, as shown in Table 1. The fluorescence quantum yields (Φ_f) from the Q bands of **1** and **2** were measured under excitation of the Soret band at 420 nm. The Φ_f of **1** and **2** were much smaller than that of **3** because of the effect of the axial amino ligand (Table 1). As the electron-donating abilities of the substituents of **2a**–**2f** got stronger, Φ_f decreased remarkably except in the case of **2c**, which exhibited a heavy atom effect. The Rehm–Weller equation (eq 1)[27] was used to predict that the free energy change (ΔG) for the electron transfer from the axial anilino ligands to the excited singlet state of the Sb(tpp) group would be negative for **2a**–**2e** using $E_{1/2}{}^{red}$, $E_{1/2}{}^{ox}$, and the excitation energy ($E^{0-0} = 2.08$ V for S_1 excitation) (Table 1). The plots of Φ_f vs ΔG showed a linear correlation (Figure 2). Recently, the decay process from the S_2 excited state of **2** under excitation of the Soret band was investigated in detail.[28] We elucidated that the charge-separation state between the axial anilino ligand and the porphyrin ring participated in the decay process from the S_2 excited state.[28] However, it was suggested that the efficiency of the internal conversion from S_2 to S_1 was the same as that of **3**, since the Φ_f of **2d** was constant under excitation of the Soret band at 420 nm and the Q band at 557 nm. Therefore, the decrease in the Φ_f of **2** can be attributed to intramolecular charge transfer from the axial amino ligand to the excited porphyrin ring in the S_1 state.

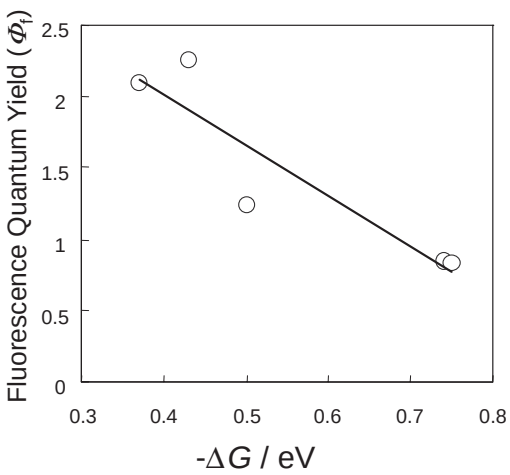

Figure 2. Plots of Φ_f vs. ΔG.

$$\Delta G = E_{1/2}{}^{ox} - E_{1/2}{}^{red} - E^{0-0}. \quad (1)$$

Effect of Protons on Fluorescence Spectra and Reduc-

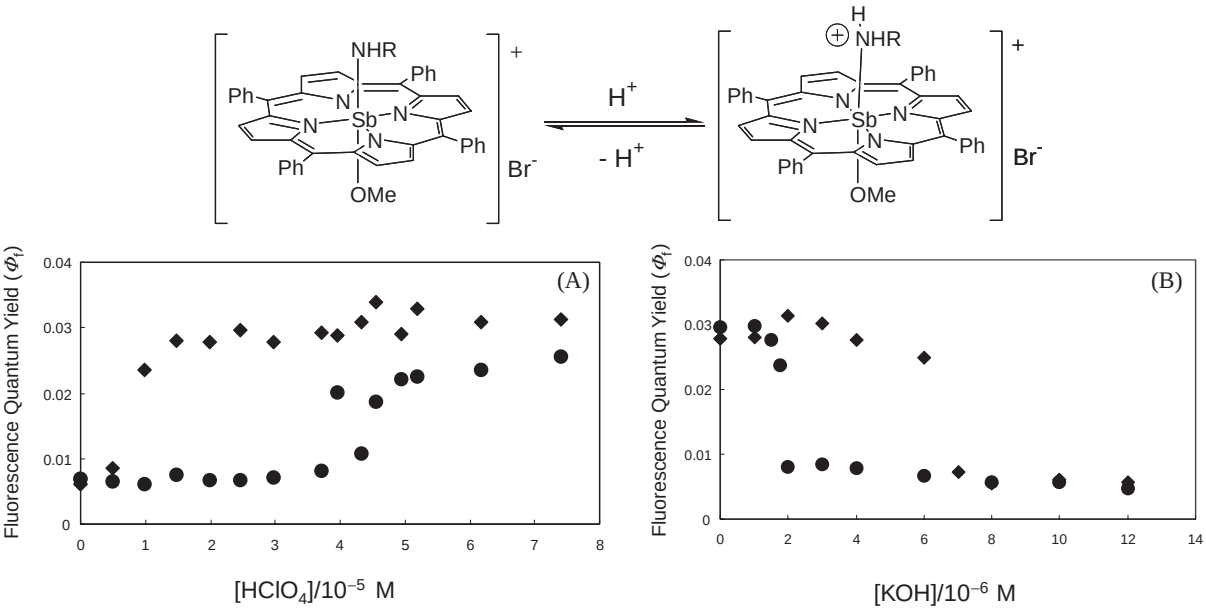

Figure 3. Plots of Φ_f for **1a** (●) and **1c** (◆) in MeCN solution with (A) the addition of $HClO_4$ and (B) the subsequent addition of KOH.

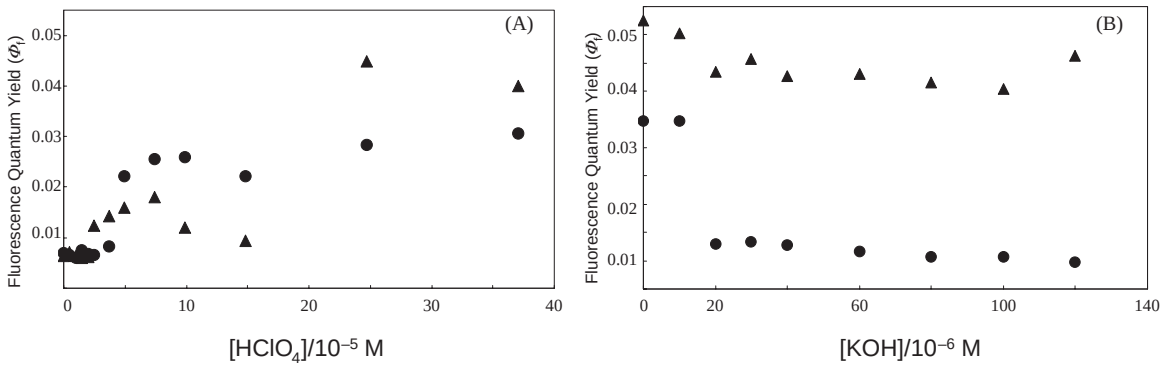

Figure 4. Plots Φ_f of **1a** (●) and **2d** (▲) in MeCN solution with (A) the addition of conc. $HClO_4$ and (B) the subsequent addition of KOH.

tion Potentials. Figure 3A shows the dependence of Φ_f on the concentration of $HClO_4$ in MeCN solutions of **1a** and **1c**. The addition of $HClO_4$ induced a hysteretic enhancement of Φ_f. Moreover, addition of an aqueous KOH solution to the acidic MeCN solutions of **1a** and **1c** led to a sharp hysteretic response of the concentration of OH^- to Φ_f, which nearly returned to its original value (Figure 3B). In the case of **3**, such fluorescence response to acid or base addition was not observed at all. It is suggested that a reversible protonation and deprotonation occurs on the lone pair on the axial nitrogen atom. Accordingly, we can easily estimate the acid dissociation constants (pK_a) for the conjugate acid of the axial amino ligand using H^+ titration curves. Thus, the pK_a values **1a**–**1f** were determined to be 4.30–5.03 (Table 1). In the case of **2d**, the addition of $HClO_4$ enhanced Φ_f, but the addition of KOH did not return to its original value (Figure 4). After titration, the formation of hydroxo(methoxo)(tetraphenylporphyrinato)antimony[13] was confirmed by mass spectroscopy measurement of the solution. Similar results were observed in all **2** with axial anilino ligands, suggesting that an acid-assisted ligand-exchange reaction is induced quantitatively.

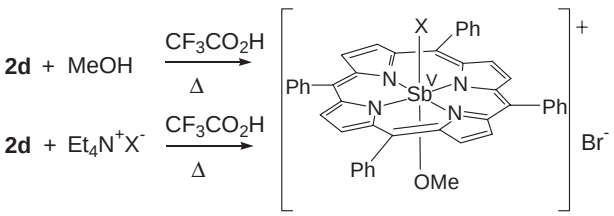

	X	Yield
6a	MeO	90%
6b	Cl	87%
5	Br	22%

Scheme 4.

Therefore, the axial ligand exchanges of **2d** with nucleophiles were performed in the presence of acid (Scheme 4). The reaction of **2d** in MeCN–MeOH (3:1 v/v) for 2 h at 50 °C in the presence of CF_3CO_2H (TFA) gave dimethoxo(tetraphenylporphyrinato)antimony(V) (**6a**)[13] in 90% yield, whereas no reaction occurred in the absence of TFA. The use of $HClO_4$ as a proton source gave the same products,

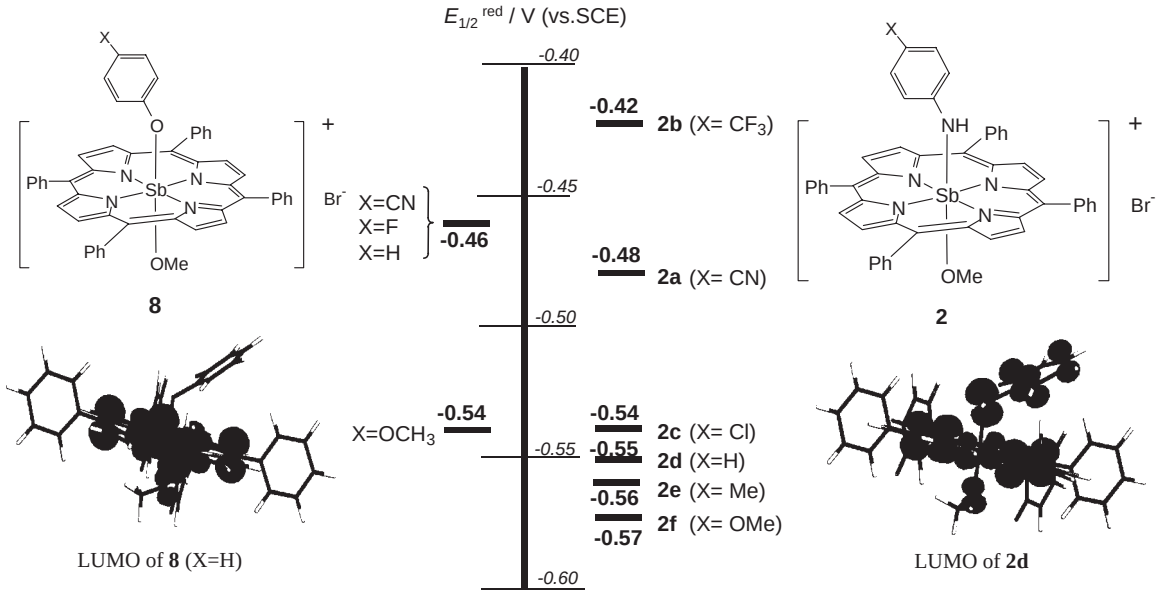

Figure 5. Comparison of the reduction potentials between **2** and **8**.

but in lower yield than in the case of TFA. Also the reaction of **2d** with $Et_4N^+Cl^-$ and $Et_4N^+Br^-$ in the presence of TFA in MeCN gave chloro(methoxo)(tetraphenylporphyrinato)antimony(V) (**6b**, 87%) and **5** (22%).[13] respectively. These results show that the protonated **2d** induced the axial ligand exchange reaction efficiently. On the other hand, the reaction of **2d** with $P(OEt)_3$ in the presence of TFA gave H_2(tpp). Moreover, absorption spectra of the reaction solution showed absorption at 465 nm due to tetraphenylporphyrinatoantimony(III) (**7**).[20] Since $P(OEt)_3$ is a good electron donor, the electron-transfer reaction from $P(OEt)_3$ to **2d** occurred efficiently, generating **7**, which gave H_2(tpp) by demetalation.

Next, we investigated the additive effect of acid on the $E_{1/2}^{red}$ of **1**. Figure 1B shows the CV of **1d** in the presence of $HClO_4$ (5.5×10^{-5} mol dm^{-3}) in MeCN. Under acidic conditions, two more reduction peaks appeared on the more positive side of **1d** (−0.28 and −0.69 V vs. SCE) than in the case of **1d** under neutral conditions. The peak current of these new reduction waves increased along with the increase in proton concentration (0–5.5×10^{-5} mol dm^{-3}). The reduction peaks observed were due to **1d** protonated on the axial nitrogen atom. The first and second reduction potentials of protonated **1d** appeared at −0.28 and −0.69 V, respectively, as irreversible peaks. On the other hand, the reduction peak of **2** was not observed under acidic conditions.

Discussion

We have previously reported the effect of an axial *p*-substituted phenoxo ligand on $E_{1/2}^{red}$ in methoxo(*p*-substituted-phenoxo)(tetraphenylporphyrinato)antimony(V) bromide (**8**).[21] In that report, the $E_{1/2}^{red}$ were little affected by the *p*-substituents on the phenoxo ligand. On the other hand, the $E_{1/2}^{red}$ of **2** depended strongly on the electron-donating or -accepting nature of the *p*-substituents (X) on the axial aniline group. The PM3 calculations of **2d** and the methoxo(phenoxo)(tetraphenylporphyrinato)antimony(V) complex (**8**; X = H) predicted the LUMO orbitals (Figure 5). The LUMO of **8** (X = H) was delocalized over the porphyrin ring, whereas the LUMO of **2d** was delocalized over both the axial anilino ligand and the porphyrin ring (Figure 5). Therefore, the energy levels of the LUMO of **2**, which are related to $E_{1/2}^{red}$, should be strongly affected by the electronic characteristics of the substituents on axial phenoxo ligands, but those of **8** should not.

Interaction between the porphyrin ring and the axial anilino ligands in a HOMO state will be the same as that in a LUMO state, judging from the spectroscopic similarities between Soret bands **1**, **2**, and **3**. Thus, these results suggest that the $E_{1/2}^{red}$ of Sb(tpp) can be controlled by the electronic effect of an axial anilino ligand.

Conclusion

The Sb(tpp)s with axial amino ligands were characterized from the viewpoint of being able to control $E_{1/2}^{red}$ and Φ_f by proton concentration and induce acid-assisted ligand exchange. It was found that the enhancement effect of Φ_f and the shifts of reduction potentials over a wide range (−0.28–−0.55 V; $\Delta E = 0.27$ V) could be induced under acidic conditions. The acid-assisted ligand exchange of **2d** with nucleophiles will provide a novel method for synthesizing Sb(tpp) complexes with various axial ligands.

Experimental

Instruments and Materials. UV–vis absorption spectra and fluorescence spectra of solutions were measured on a Hitachi U2001 spectrometer and on a Hitachi F4500 spectrometer, respectively. ^{1}H NMR spectra were taken in $CDCl_3$ using Me_4Si as an internal standard on a Bruker AC 250P spectrometer at 250 MHz. SIMS spectra were obtained on a Hitachi M-2000AM spectrophotometer. The PM3 calculation was performed on a Silicon graphics O2 work station using the SPARTAN program. All chemicals were of the best commercial grades available.

Synthesis of Amino(methoxo)(tetraphenylporphyrinato)-antimony(V) Complexes 1–3. According to a reported method,[29] **3** and **5** were prepared by the reaction of **4** with H_2O and

MeOH, respectively. An MeCN–pyridine solution (5:1 v/v 50 mL) containing **5** (1.1 mmol) and aliphatic amines or 4-substituted aniline derivatives was heated for 4 h at 80 °C. The solvent was evaporated and the residue was dissolved in CH_2Cl_2. The CH_2Cl_2 solution was washed three times with 50 mL portions of H_2O. After evaporation, the crude product was chromatographed on silica gel (Fuji Silysia BW-300) using $CHCl_3$–MeOH (10:1 v/v) as an eluent to give **1** and **2**. The spectral data of **1a–1f** are shown below. On ^{1}H NMR measurements, peaks of NH proton in **1** and **2** were not all observed due to extremely broad lines. The spectral data of **2a–2e** have been reported in recent literature.[28]

Benzylamino(methoxo)(tetraphenylporphyrinato)antimony(V) Bromide (1a): Yield 73% from **5**; SIMS: m/z 869 (M^+); ^{1}H NMR ($CDCl_3$) δ −2.47 (3H, s, Sb-OCH_3), −1.39 (2H, s, Sb–NH–CH_2–), 4.27 (2H, d, $J = 7.2$ Hz, axial Ph), 6.42 (1H, m, axial Ph), 6.65 (2H, t, $J = 7.3$ Hz, axial Ph), 7.82–7.94 (12H, m, Ph), 8.24 (4H, d, $J = 6.9$ Hz, Ph), 8.41 (4H, d, $J = 6.4$ Hz, Ph), 9.38 (8H, s, pyrrole).

3-Hydroxypropylamino(methoxo)(tetraphenylporphyrinato)antimony(V) Bromide (1b): Yield 70% from **5**; SIMS: m/z 837 (M^+); ^{1}H NMR ($CDCl_3$) δ −2.84 (2H, t, $J = 7.0$ Hz, Sb–NH–CH_2–), −2.43 (3H, s, Sb–OCH_3), −1.57 (2H, quint, $J = 7.0$ Hz, –CH_2–), 1.28 (2H, t, $J = 7.4$ Hz, –CH_2–OH), 7.85–7.91 (12H, m, Ph), 8.27 (4H, d, $J = 6.4$ Hz, Ph), 8.55 (4H, d, $J = 6.4$ Hz, Ph), 9.41 (8H, s, pyrrole).

Butylamino(methoxo)(tetraphenylporphyrinato)antimony(V) Bromide (1c): Yield 73% from **5**; SIMS: m/z 836 ($M^+ - 1$); ^{1}H NMR ($CDCl_3$) δ −3.09 (2H, t, $J = 7.0$ Hz, Sb–NH–CH_2–), −2.43 (3H, s, Sb–O–CH_3), −1.82 (2H, quint, $J = 7.0$ Hz, –CH_2–), −1.08 (2H, hex, $J = 7.4$ Hz, –CH_2–), −0.41 (3H, t, $J = 7.4$ Hz, –CH_3), 7.82–7.94 (12H, m, Ph), 8.24 (4H, d, $J = 6.4$ Hz, Ph), 8.41 (4H, d, $J = 6.4$ Hz, Ph), 9.38 (8H, s, pyrrole).

Isopropylamino(methoxo)(tetraphenylporphyrinato)antimony(V) Bromide (1d): Yield 76% from **5**; SIMS: m/z 821 ($M^+ - 1$); ^{1}H NMR ($CDCl_3$) δ −3.88 (1H, m, Sb–NH–CH–), −2.42 (3H, s, Sb–OCH_3), −1.99 (6H, d, $J = 6.2$ Hz, –$CH(CH_3)_2$), 7.89–7.96 (12H, m, Ph), 8.29 (4H, d, $J = 6.4$ Hz, Ph), 8.38 (4H, d, $J = 6.4$ Hz, Ph), 9.45 (8H, s, pyrrole).

***tert*-Butylamino(methoxo)(tetraphenylporphyrinato)antimony(V) Bromide (1e):** Yield 73% from **5**; SIMS: m/z 835 ($M^+ - 1$); ^{1}H NMR ($CDCl_3$) δ −2.57 (3H, s, Sb–OCH_3), −2.46 (9H, s, Sb–NH–$C(CH_3)_3$), 7.91–7.96 (12H, m, Ph), 8.30 (4H, d, $J = 6.7$ Hz, Ph), 8.39 (4H, d, $J = 6.8$ Hz, Ph), 9.48 (8H, s, pyrrole).

Pyperidino(methoxo)(tetraphenylporphyrinato)antimony(V) Bromide (1f): Yield 31% from **5**; SIMS: m/z 846 (M^+); ^{1}H NMR ($CDCl_3$) δ −3.32 (4H, t, $J = 7.0$ Hz, Sb–NH–$(CH_2)_2$–), −2.43 (3H, s, Sb–OCH_3), −1.57 (4H, quint, $J = 7.0$ Hz, –$(CH_2)_2$–), −0.52 (2H, quint, $J = 7.3$ Hz, –CH_2–), 7.89–7.96 (12H, m, Ph), 8.29 (4H, d, $J = 6.2$ Hz, Ph), 8.38 (4H, d, $J = 6.4$ Hz, Ph), 9.48 (8H, s, pyrrole).

Reaction of 2d with Nucleophiles in the Presence of CF_3CO_2H. The reaction of **2d** (0.01 mmol) in MeCN–MeOH (9:1, 20 mL) in the presence of CF_3CO_2H (0.18 mmol) for 2 h at 50 °C gave **6a**[13] in 90% yield. The reaction of **2d** (0.01 mmol) with $Et_4N^+Cl^-$ and $Et_4N^+Br^-$ (0.01 mmol) in the presence of CF_3CO_2H (0.18 mmol) gave **6b** and **5**[29] in 87% and 27% yields, respectively.

Chloro(methoxo)(tetraphenylporphyrinato)antimony(V) Bromide (6b): Yield 87% from **2d**. SIMS: m/z 800 (M^+); ^{1}H NMR ($CDCl_3$) δ −2.04 (3H, s, Sb–OCH_3), 7.94–8.02 (12H, m, Ph), 8.35 (4H, d, $J = 6.4$ Hz, Ph), 8.42 (4H, d, $J = 6.4$ Hz, Ph), 9.58 (8H, s, pyrrole).

Fluorescence Quantum Yields. The concentrations of **1** and **2** in MeCN solutions were adjusted for the absorbance to be less than 0.1 at the excitation wavelength (420 nm). The fluorescence quantum yields (Φ_f) were determined by using an MeCN solution of **3** ($\Phi_f = 0.0518$) as an actinometer.[13] The acid dissociation constants (pK_a) for the conjugated acid of axial amino ligand of **1** were estimated from a proton concentration at the half of the maximum fluorescence intensity.

Measurements of Redox Potentials. The oxidation and reduction potentials of a dried MeCN solution of **1–3** (1×10^{-2} mol dm^{-3}) in the presence of a supporting electrolyte (Et_4NBF_4; 0.1 mol dm^{-3}) were measured by cyclic voltammetry at a scan rate of 300–500 mV s^{-1} at 25 °C on a BAS CV-50W cyclic voltammeter using a carbon-disk working electrode, a Pt counter electrode, and an $Ag/AgNO_3$ reference electrode. The half-peaks of the oxidation ($E_{1/2}^{ox}$) and reduction potentials ($E_{1/2}^{red}$) vs Ag/Ag^+ were modified to those vs. SCE by the addition of +0.22 V.

X-ray Crystallographic Analysis. The structure of **1b** was determined unambiguously by X-ray crystallographic analysis on an Enraf Nonius CAD-4 system using Mo Kα irradiation ($\lambda = 0.7107$ Å).

1b: $C_{48}H_{39}N_5O_2SbBr$, $M_r = 919$, monoclinic, $P2_1$ (space group number 4), $a = 12.7088$ Å, $b = 12.2072$ Å, $c = 15.4114$ Å, $\beta = 106.7°$, $V = 2290$ Å^3, $Z = 2$, $D_{calcd} = 1.31$ g cm^{-3}, $D_m = 1.33$ g cm^{-3}, $R = 0.0777$, $R_w = 0.0863$. The molecular structure of **1b** was drawn using Chem 3D based on X-ray crystallographic data (Scheme 3). Crystallographic data reported in this manuscript have been deposited with Cambridge Crystallographic Data Centre as supplementary publication No. CCDC-677875. Copies of the data can be obtained free of charge via http://www.ccdc.cam.ac.uk/conts/retrieving.html (or from the Cambridge Crystallographic Data Centre, 12, Union Road, Cambridge, CB2 1EZ, UK; fax: +44 1223 336033; or deposit@ccdc.cam.ac.uk).

This research was supported by a Grant-in-Aid for Scientific Research (No. 19550068, No. 16550127, and No. 17029053 Scientific Research in Priority Areas 417) from the Ministry of Education, Culture, Sports, Science and Technology. We are grateful to Prof. H. Inoue (Tokyo Metropolitan University) for additional financial support (SORST from Japan Science and Technology Agency).

References

1 *The Porphyrin Handbook*, ed. by D. Gust, T. A. Moore, K. M. Kadish, K. M. Smith, R. Guilard, Academic Press, New York, **2000**, Vol. 8, p. 153, and references cited therein.

2 K. Kalyanasundaram, M. Grätzel, *Photosensitization and Photocatalysis using Inorganic and Organometallic Compounds*, Kluwer Academic Publishers, Amsterdam, **1993**.

3 A. Harriman, P. Neta, C. M. Richoux, in *Homogeneous and Heterogeneous Photocatalysis*, ed. by E. Pelizzetti, N. Serpone, Reidel, Dordrecht, **1986**, p. 123, and references cited therein.

4 U. Bach, D. Lupo, P. Comte, J. Moser, F. Weissortel, J. Salbeck, H. Spreitzer, M. Grätzel, *Nature* **1998**, *395*, 583.

5 W. M. Campbell, A. K. Burrell, D. L. Officer, K. W. Jolley, *Coord. Chem. Rev.* **2004**, *248*, 1363.

6 Y. Yamamoto, K.-Y. Akiba, *J. Organomet. Chem.* **2000**, *611*, 200.

7 K.-Y. Akiba, in *The Chemistry of Hypervalent Compounds*, ed. by K.-Y. Akiba, Wiley-VCH, U.K., **1999**, Chap. 1.
8 N. Nakamoto, K.-Y. Akiba, *J. Am. Chem. Soc.* **1999**, *121*, 6958.
9 C. Cloutour, D. Lafargue, J. C. Pommier, *J. Organomet. Chem.* **1978**, *161*, 327.
10 C. Cloutour, D. Lafarque, J. C. Pommier, *J. Organomet. Chem.* **1980**, *190*, 35.
11 T. Shiragami, K. Kubomura, D. Ishibashi, H. Inoue, *J. Am. Chem. Soc.* **1996**, *118*, 6311.
12 S. Takagi, M. Suzuki, T. Shiragami, H. Inoue, *J. Am. Chem. Soc.* **1997**, *119*, 8712.
13 T. Shiragami, J. Matsumoto, H. Inoue, M. Yasuda, *J. Photochem. Photobiol., C* **2005**, *6*, 227.
14 T. Barbour, W. J. Belcher, P. J. Brothers, C. E. F. Rickard, D. C. Ware, *Inorg. Chem.* **1992**, *31*, 746.
15 K. M. Kadish, M. Autret, Z. Ou, K.-Y. Akiba, S. Matsumoto, R. Wada, Y. Yamamoto, *Inorg. Chem.* **1996**, *35*, 5564.
16 I.-C. Liu, J.-H. Chen, S.-S. Wang, J.-C. Wang, *Polyhedron* **1996**, *15*, 3947.
17 T. Ogawa, H. Furuta, M. Takahashi, A. Morino, H. Uno, *J. Organomet. Chem.* **2000**, *611*, 511.
18 G. Knor, *Coord. Chem. Rev.* **1998**, *171*, 61.
19 G. Knor, *Inorg. Chem. Commun.* **2000**, *3*, 505.
20 G. Knor, *Chem. Phys. Lett.* **2000**, *330*, 383.
21 T. Shiragami, Y. Andou, Y. Hamasuna, F. Yamaguchi, K. Shima, M. Yasuda, *Bull. Chem. Soc. Jpn.* **2002**, *75*, 1577.
22 W. Satoh, S. Masumoto, M. Shimizu, Y. Yamamoto, K.-Y. Akiba, *Bull. Chem. Soc. Jpn.* **1999**, *72*, 459.
23 H. Segawa, K. Kunimoto, A. Nakamoto, T. Shimidzu, *J. Chem. Soc., Perkin Trans. 1* **1992**, 939.
24 Y. Yamamoto, R. Nadano, M. Itagaki, K.-Y. Akiba, *J. Am. Chem. Soc.* **1995**, *117*, 8287.
25 K. M. Kadish, Q. Y. Xu, J.-M. Barbe, J. E. Anderson, E. Wang, R. Guilard, *J. Am. Chem. Soc.* **1987**, *109*, 7705.
26 D. Y. Dawson, J. C. Sangalang, J. Arnold, *J. Am. Chem. Soc.* **1996**, *118*, 6082.
27 D. Rehm, A. Weller, *Isr. J. Chem.* **1970**, *8*, 259.
28 M. Fujitsuka, D. W. Cho, T. Shiragami, M. Yasuda, T. Majima, *J. Phys. Chem. B* **2006**, *110*, 9368.
29 T. Shiragami, K. Tanaka, Y. Andou, S. Tsunami, J. Matsumoto, H. Luo, Y. Araki, O. Ito, H. Inoue, M. Yasuda, *J. Photochem. Photobiol., A* **2005**, *170*, 287.